

Hadronic matter form factors: pp , πp , and the valon model

S. Sanielevici and P. Valin

Physics Department, McGill University, Montreal, Quebec H3A 2T8, Canada

(Received 10 June 1983)

We define the "matter form factor" (MFF) in hadron-hadron elastic scattering as the Fourier-Bessel transform of the eikonal. The MFF's for pp and πp are extracted directly from the measured differential cross sections. We show that the valon model is a convenient framework in which these form factors can be analyzed and related to each other.

I. INTRODUCTION

It is a nice feature of impact-parameter pictures of hadron-hadron scattering that they connect the measured observables to the geometric and dynamic structure of the colliding hadrons.¹⁻³ Clearly, what we see in hadron-hadron collisions at present energies cannot simply be identified with electromagnetic form factors as measured in lepton-hadron elastic scattering. Rather, hadron-hadron elastic scattering defines its own form factor through the impact-parameter formalism. This "matter form factor" (MFF) measures the interaction of a gluonic probe with the excited matter of the overlapping hadrons and should incorporate the static matter distribution of the participating hadrons as well as the dynamical modes of excitation of hadronic matter during the high-energy collision.

The "valon model"⁴⁻⁷ is an attractive picture of hadron structure, consistent with a large body of experimental facts and theoretical findings in hard and soft hadronic processes, in perturbative and nonperturbative QCD.⁸ It has produced explicit and simple expressions for charge and matter distributions in nucleons and pions at low and moderate Q^2 . Since the charge distributions have been applied successfully to the study of charge form factors in Ref. 7, it seems worthwhile to investigate whether the matter distributions can be analogously related to MFF's. In particular, we wish to predict the πp MFF from the "experimental" pp MFF, similarly to the valon-model prediction of the pion charge form factor from the proton charge form factor.⁷ Of course, the valon-model description of charge form factors will have to be suitably generalized to accommodate the complicated central-region dynamics in hadron-hadron scattering.

II. DEFINITIONS AND ASSUMPTIONS

Consider elastic scattering of hadrons A and B at energies which are sufficiently high for the differential cross section to be well described by the spin-nonflip, purely absorptive scattering amplitude $f(s, t)$ (Ref. 9):

$$\frac{d\sigma}{dt} = \pi |f(s, t)|^2 \quad (1)$$

(s is the c.m. energy squared, t the four-momentum transfer squared, and $Q^2 = -t$). The impact-parameter representation is defined by the inverse Fourier-Bessel

transform of f :

$$f(s, t) = i \int_0^\infty h(s, b) J_0(b\sqrt{-t}) b db \quad (2)$$

with $h(s, b)$ purely real. s -channel unitarity relates it to the inelastic overlap function $G(s, b)$:

$$h(s, b) = 1 - [1 - G(s, b)]^{1/2}. \quad (3)$$

The eikonal Ω is defined from h by the relation

$$\Omega(s, b) = -\ln[1 - h(s, b)]. \quad (4)$$

Using (3), it can also be expressed in terms of G :

$$\Omega(s, b) = -\frac{1}{2} \ln[1 - G(s, b)]. \quad (5)$$

We are now ready to define the "MFF of the system AB " as the Fourier-Bessel transform of the eikonal (normalized to unity in the forward direction):

$$M_{AB}(s, t) = \frac{\int_0^\infty \Omega(s, b) J_0(b\sqrt{-t}) b db}{\int_0^\infty \Omega(s, b) b db}. \quad (6)$$

Our working hypothesis is that this quantity can be calculated in the valon model. We generalize the valon-model ansatz for charge form factors^{5,7} to an ansatz for the MFF:

$$M_{AB}(s, t) = K_A(Q^2) K_B(Q^2) V(s, Q^2), \quad (7)$$

where K_A, K_B give the contribution of structureless valons to the host hadrons' MFF while V is the valon-valon ("reduced") MFF. Note that the MFF is not positive-definite in either (6) or (7).

The reduced MFF is a complicated object, some intricate combination of the bound-state structure of the colliding valons and of its dynamical excitations. It is not yet calculable. However, since the internal structure of valons is built by virtual QCD processes only, it ought to be the same for all flavors of valons and also be independent of the host hadron. We can therefore expect valon-model universality,⁷ but only modulo the unknown dynamical part of the reduced MFF. In fact, our results presented below suggest there exist "equivalent energies" at which MFF's for different hadron-hadron systems are related by valon-model universality.

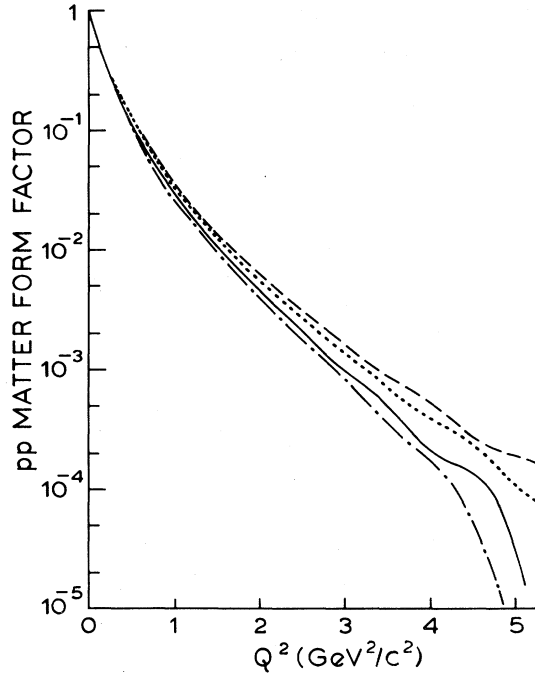


FIG. 1. The pp matter form factor from overlap data at four ISR energies. Dotted curve at $\sqrt{s} = 23.5$ GeV, dashed curve at $\sqrt{s} = 30.7$ GeV, dash-dotted curve at $\sqrt{s} = 44.7$ GeV, and solid curve at $\sqrt{s} = 52.8$ GeV.

III. THE pp MFF

We have used two methods to extract the pp MFF from experimental data. The input to the first is the tabulation of $G(s, b)$ by Amaldi and Schubert.¹⁰ We transform to eikonal values according to (5), performing a natural cubic 60-node spline at each CERN ISR energy. Then we extract M_{pp} by (6), using a double-precision 32-point Gaussian quadrature between Bessel-function zeros. The results for four ISR energies are shown in Fig. 1. We have not included the top ISR energy because the resulting MFF had violent oscillations, probably due to several questionable data points signaled in Ref. 11. This numerical method can only be trusted up to $-t = 5$ (GeV/c)².

To do better, we fit the pp differential cross section as measured at the ISR for $\sqrt{s} = 52.8$ GeV,¹² and at Fermilab for $p_{\text{lab}} = 400$ GeV/c and large $-t$.¹³ We need the

TABLE I. Parameters for fits to the pp and πp differential cross sections [Eq. (8)]. A_j is in (mb)^{1/2} (GeV/c)⁻¹, B_j in (GeV/c)⁻².

j	pp		πp	
	A_j	B_j	A_j	B_j
1	0.606 66	15.042	1.8075	6.4557
2	3.2310	6.6985	1.2652	2.8597
3	1.6289	3.8590	0.035 29	1.0190
4	-0.034 43	1.0353	-0.00426	0.427 99
5	-0.000 799	0.380 62		

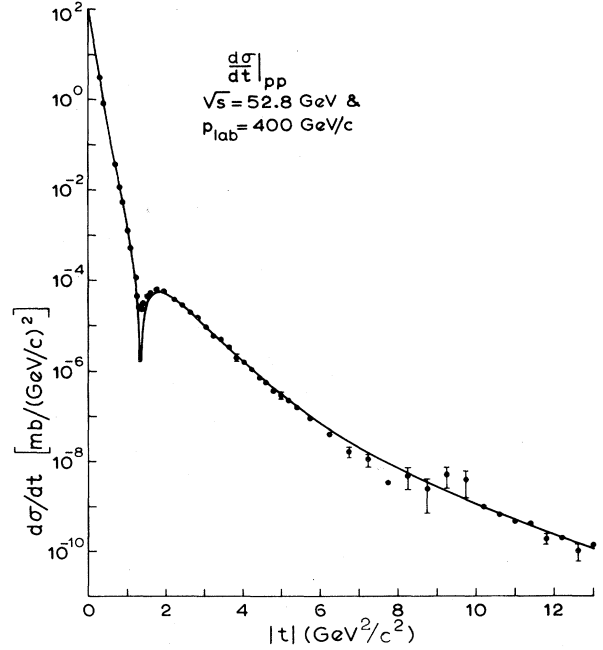


FIG. 2. Five-exponential fit to the pp differential cross section. Data are from the ISR at $\sqrt{s} = 52.8$ GeV and from Fermilab at $p_{\text{lab}} = 400$ GeV/c and large $-t$. Typical error bars are shown.

large $-t$ data to improve the numerical Fourier-Bessel transform. Generalizing a form used in Ref. 9, we set

$$f(s, t) = i \sum_{j=1}^J A_j e^{B_j t} \quad (8)$$

with $J=5$. A_j and B_j as obtained using the CERN MINUIT routine are listed in Table I. The fit is shown in Fig. 2. We perform the Fourier-Bessel transform of the eikonal obtained from (8) and get an independent extraction of the pp MFF. The result as compared to the extraction by method 1 for the same s, Q^2 is shown in Fig. 3.

Method 2 should give a reliable idea of the larger- Q^2 behavior of the pp MFF. In our fit, which does not have multiple diffraction zeros, the MFF goes negative at $Q_0^2 = 5.65$ (GeV/c)². This confirms previous findings.^{2,14} Q_0^2 would be different for different s .

We can now establish the relevance of the valon model to the pp MFF. For the proton, we use

$$K_p(Q^2) = \frac{1}{3} \int_0^1 dx [2L_p^U(x)T_p^U(\vec{K}) + L_p^D(x)T_p^D(\vec{K})] |_{\vec{K}=(1-x)\vec{Q}} \quad (9)$$

Here, L_p^U (L_p^D) are the longitudinal-momentum-fraction distributions of U (D) valons in the proton⁶

$$L_p^U(x) = 7.98x^{0.65}(1-x)^2, \quad (10)$$

$$L_p^D(x) = 6.01x^{0.35}(1-x)^2,$$

and T_p^U (T_p^D) are the transverse-momentum distributions of U (D) valons in the proton⁷

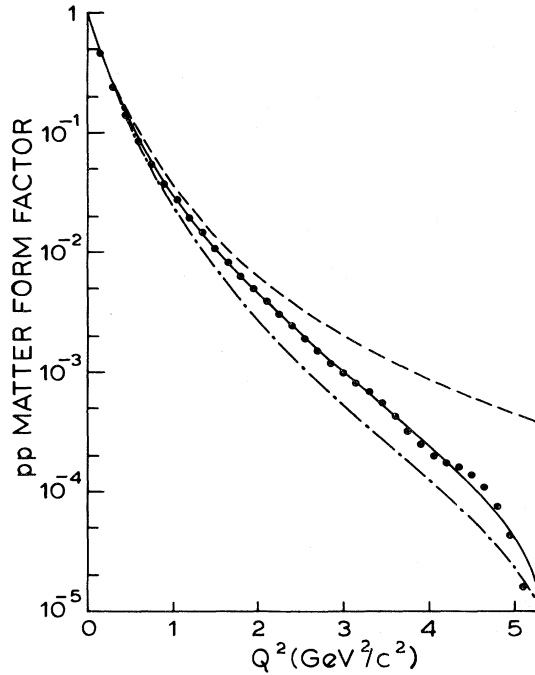


FIG. 3. pp matter form factors by various methods at $\sqrt{s} = 52.8$ GeV and for $Q^2 < 5.3$ (GeV/c)². The points reproduce the solid curve of Fig. 1. Solid curve: extraction by method 2. Dashed curve: Eq. (9) squared. Dash-dotted curve: Eq. (12).

$$T_p^U(\vec{K}) = e^{-6.1K^2}, \quad T_p^D(\vec{K}) = e^{-3K^2}. \quad (11)$$

The square of quantity (9) is represented by the dashed curve in Fig. 3. An immediate way to come closer to the experimental MFF is to multiply it by a factor of the form suggested in Ref. 2 (BSW)

$$M_{pp} \approx K_p^2(Q^2) \frac{a^2 - Q^2}{a^2 + Q^2}, \quad (12)$$

where a^2 would now be s -dependent in principle. The dash-dotted curve in Fig. 3 is obtained by fixing the parameter a^2 to Q_0^2 . A future theory of the reduced MFF might justify one to untie a^2 from the exact value of the experimental zero, making it a free parameter to actually fit the extracted MFF. For instance, $a^2 = 7$ (GeV/c)² yields a good fit to the extracted MFF shown in Fig. 3 [$Q^2 < 5.2$ (GeV/c)²].

The coefficients in (11) are from Ref. 7 (simultaneous fit to p, n, π charge form factors), but in (10) we prefer to use coefficients from Ref. 6 (fit to structure functions determined from μN and νN deep-inelastic-scattering data at high Q^2). Using coefficients from Ref. 7 in the longitudinal distributions does not make much difference, but the resulting approximation (12) is somewhat worse.

IV. THE πp MFF

Let us assume that we work at equivalent c.m. energies for pp and πp elastic scattering. Taking approximation

(12) as an illustrative example, this would mean that we can write

$$M_{pp} = K_p^2 \frac{a^2 - Q^2}{a^2 + Q^2}, \quad (13)$$

$$M_{\pi p} = K_\pi K_p \frac{a^2 - Q^2}{a^2 + Q^2} \quad (14)$$

with the same value of a^2 . But even though the reduced MFF is only approximated by the BSW factor, the mere hypothesis of its universality at equivalent energies along with the factorized ansatz (7) allows us to eliminate it between the MFF's for the two systems. Therefore, knowledge of the experimental pp MFF should enable us to predict the πp MFF by the formula

$$M_{\pi p} = \left[\frac{K_\pi}{K_p} \right] M_{pp}. \quad (15)$$

We take our pp MFF extracted by method 2 at $\sqrt{s} = 52.8$ GeV as representative of the ISR regime and predict a πp MFF which should not be far from what can be extracted directly from the πp differential cross section at $p_{\text{lab}} = 200$ GeV/c (the energy at which diffractive structure appears in πp scattering). For the pion MFF due to structureless valons we take

$$\begin{aligned} K_\pi(Q^2) &= \int_0^1 dx L_\pi(x) T_\pi(\vec{K}) \Big|_{\vec{K} = (1-x)\vec{Q}}, \\ L_\pi(x) &= 1.77x^{0.3}(1-x)^{0.3}, \\ T_\pi(\vec{K}) &= e^{-6K^2}. \end{aligned} \quad (16)$$

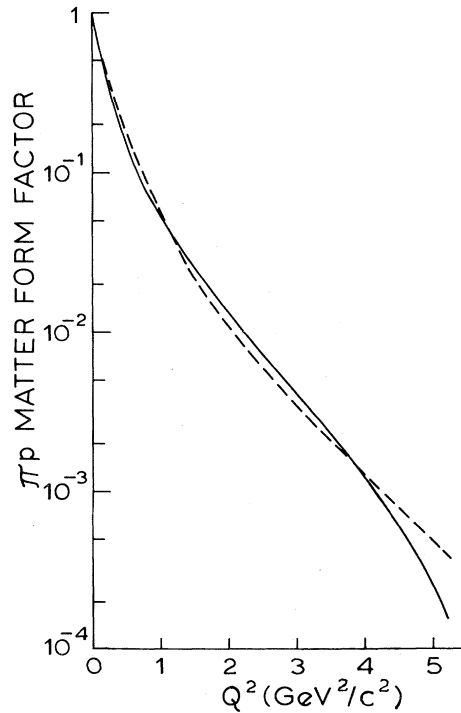


FIG. 4. The πp matter form factor. Solid curve: prediction from the pp MFF extracted at $\sqrt{s} = 52.8$ GeV. Dashed curve: direct extraction from Fermilab data at $p_{\text{lab}} = 200$ GeV/c .

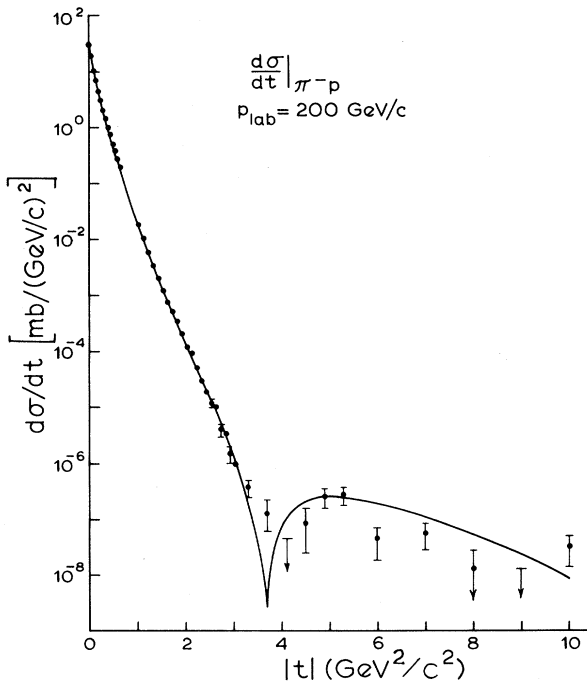


FIG. 5. Four-exponential fit to the πp differential cross section. Data from Fermilab at $p_{\text{lab}}=200$ GeV/c. Typical error bars are shown.

The resulting prediction is the full curve in Fig. 4.

To check our prediction, we extract the πp MFF directly from π^-p data on the differential cross section taken at Fermilab for $p_{\text{lab}}=200$ GeV/c (Refs. 15 and 16). The value at the optical point is calculated from the total cross section given in Ref. 17. We use method 2 with a four-exponential form for the scattering amplitude [$J=4$ in Eq. (8)]. The fit is shown in Fig. 5, the parameters are given in Table I, and the result for the πp MFF is the dashed curve in Fig. 4.

The agreement is good up to $Q^2 \cong 5$ (GeV/c) 2 . The “experimental” MFF goes negative at $Q_1^2=8.5$ (GeV/c) 2 , whereas our prediction inherits the $Q_0^2=5.65$ (GeV/c) 2 from the pp MFF. This is the only source of disagreement and indicates that $p_{\text{lab}}=200$ GeV/c for πp is not quite equivalent to $\sqrt{s}=52.8$ GeV for pp , but of the same order. In fact, it is easy to verify that Eq. (14) with $a^2=8.5$ (GeV/c) 2 is a good approximation to the “experimental” πp MFF, and that Eq. (13) with this value of a^2 yields a pp MFF which is nearly the median of the curves in Fig. 1.

As is apparent from Figs. 2 and 5, our sum-of-exponential fits to differential cross sections never have multiple diffraction dips. At the same time, they lead to

TABLE II. Parameters for fit of Eq. (17) to the πp differential cross section following Ref. 18. All parameters are in (GeV/c) $^{-2}$.

α_1	2.863	β_1	6.120
α_2	2.038	β_2	2.886
α_3	0.01265	β_3	0.4467
γ	0.6237		

MFF’s which go negative at relatively low values of Q^2 . If one interprets the πp data point at $-t=9$ (GeV/c) as a second dip, for instance, by fitting with the form proposed in Ref. 18,

$$f_{\pi p}(s,t) = \alpha_1 e^{\beta_1 t} + \alpha_2 e^{\beta_2 t} + \alpha_3 e^{\beta_3 t} J_0(-\gamma t) \quad (17)$$

(their coefficients are reproduced in Table II), then one obtains a πp MFF which is nearly identical to our extraction in the Q^2 range shown in Fig. 4, but stays positive up to $Q^2=20$ (GeV/c) 2 . This is why we never show any MFF’s beyond 5 (GeV/c) 2 : we feel one should first gain some theoretical understanding of the behavior of (reduced) MFF’s in that region. At any rate, there definitely seems to be a link between this problem and the question of further diffraction dips.

V. CONCLUSIONS

In this paper we have displayed the s and low- Q^2 dependence of the pp MFF within the ISR regime. The good agreement between two independent methods gives us confidence in the extracted form factors. Therefore we also extract the πp MFF from Fermilab data at $p_{\text{lab}}=200$ GeV/c.

Our working hypothesis of identifying the MFF defined in the impact-parameter formalism with a generalization of the valon-model ansatz for charge form factors has produced interesting results. The products of MFF’s due to the distributions of structureless valons in p and π by the BSW factor approximate the extracted pp and πp MFF’s quite well. The fact that valon-model factorizability and universality allow a close prediction of the πp MFF from the pp MFF and vice versa indicates that these hypotheses are correct modulo the energy dependence of the reduced (valon-valon) MFF, which thereby becomes an object of considerable physical interest.

ACKNOWLEDGMENTS

The authors wish to acknowledge useful discussions with R. Henzi and C. S. Lam. This work was supported in part by the Natural Sciences and Engineering Research Council of Canada and the Department of Education of the Province of Québec.

¹T. T. Chou and C. N. Yang, Phys. Rev. **170**, 5 (1968).

²C. Bourrely, J. Soffer, and T. T. Wu, Phys. Rev. D **19**, 3249 (1979).

³H. I. Miettinen and G. H. Thomas, Nucl. Phys. **B166**, 365 (1980).

⁴R. C. Hwa, Phys. Rev. D **22**, 759 (1980).

⁵For a review, see R. C. Hwa, in *Partons in Soft Hadronic Processes*, proceedings of the Europhysics Conference, Erice, Italy, 1981, edited by R. T. van de Walle (World Scientific, Singapore, 1981).

- ⁶R. C. Hwa and M. S. Zahir, Phys. Rev. D 23, 2539 (1981); 25, 2455 (1982).
- ⁷R. C. Hwa and C. S. Lam, Phys. Rev. D 26, 2338 (1982).
- ⁸For links to nonperturbative QCD, see, e.g., E. V. Shuryak, Nucl. Phys. B203, 93 (1982); B203, 116 (1982); B203, 140 (1982).
- ⁹R. Henzi and P. Valin, Nucl. Phys. B148, 513 (1979).
- ¹⁰U. Amaldi and K. R. Schubert, Nucl. Phys. B166, 301 (1980).
- ¹¹P. Valin, Nucl. Phys. B218, 215 (1983).
- ¹²K. R. Schubert, in *Landolt-Börnstein: Numerical Data and Functional Relationships in Science and Technology*, edited by K.-H. Hellwege (Springer, Berlin, 1979), New Series, Group I, Vol. 1.
- ¹³S. Conetti *et al.*, Phys. Rev. Lett. 41, 924 (1978).
- ¹⁴V. Franco, Phys. Rev. D 11, 1837 (1975).
- ¹⁵A. Schiz *et al.*, Phys. Rev. D 24, 26 (1981).
- ¹⁶W. F. Baker *et al.*, Phys. Rev. Lett. 47, 1683 (1981).
- ¹⁷A. S. Carroll *et al.*, Phys. Lett. 80B, 423 (1979).
- ¹⁸C. H. Lai, S. Y. Lo, and K. K. Phua, Phys. Rev. D 27, 2214 (1983).